

# SWIFT: Fast algorithms for multi-resolution SPH on multi-core architectures

Pedro Gonnet<sup>\*</sup>, Matthieu Schaller<sup>†</sup>, Tom Theuns<sup>†‡</sup>, Aidan B. G. Chalk<sup>\*</sup>

<sup>\*</sup>School of Engineering and Computing Sciences,  
Durham University,  
DH1 3LE Durham, UK  
{pedro.gonnet,aidan.chalk}@durham.ac.uk

<sup>†</sup>Institute for Computational Cosmology,  
Durham University,  
DH1 3LE Durham, UK  
{matthieu.schaller,tom.theuns}@durham.ac.uk

<sup>‡</sup>Department of Physics,  
University of Antwerp, Groenenborgerlaan 171,  
B-2020 Antwerp, Belgium

**Abstract**—This paper describes a novel approach to neighbour-finding in Smoothed Particle Hydrodynamics (SPH) simulations with large dynamic range in smoothing length. This approach is based on hierarchical cell decompositions, sorted interactions, and a task-based formulation. It is shown to be faster than traditional tree-based codes, and to scale better than domain decomposition-based approaches on shared-memory parallel architectures such as multi-cores.

## I. INTRODUCTION

Since the past few years, due to the physical limitations on the speed of individual processor cores, instead of getting *faster*, computers are getting *more parallel*. This increase in parallelism comes mainly in the form of *multi-core* computers in which the number cores can be expected to continue growing exponentially, e.g. following Moore's law, much in the same way processor speeds were up until a few years ago.

The predominant paradigm for parallel computing is currently distributed-memory parallelism using MPI (Message Passing Interface) [1], in which large simulations are generally parallelized by means of data decompositions, i.e. by assigning each node or core a portion of the data on which to work. The cores execute the same code in parallel, each on its own part on the data, intermittently exchanging data. The amount of *computation* local to the node is then proportional to the amount of data it contains, e.g. its volume, while the amount of *communication* is proportional to the amount of computation spanning two or more nodes, e.g. its surface. If the number of nodes increases, or smaller problems are considered, the surface-to-volume ratio, i.e. the ratio of communication to computation, grows, and the time spent on communication will increasingly dominate the entire simulation, reducing scaling and parallel efficiency.

Assuming the individual cores do not get any faster, this

means that small simulations, for which the maximum degree of parallelism has already been reached, will never become any faster. In order to speed up small simulations, or to continue scaling for large simulations, new approaches on how computations are parallelized need to be considered.

With the above in mind, we will, in the following, describe a reformulation of the underlying algorithms for Smoothed Particle Hydrodynamics (SPH) simulations which uses asynchronous task-based shared-memory parallelism to achieve better parallel scaling and efficiency on multi-core architectures.

## II. ALGORITHMS

The interactions in compressible gas dynamics using SPH are computed in two distinct stages that are evaluated separately:

- 1) *Density* computation: For each particle  $p_i$ , loop over all particles  $p_j$  within  $h_i$  of  $p_i$  and compute the particle densities.
- 2) *Force* computation: For each particle  $p_i$ , loop over all particles  $p_j$  within  $\max\{h_i, h_j\}$  and compute the particle forces.

The identification of these interacting particle pairs incurs the main computational cost, as will be shown in the following sections, and therefore also presents the main challenge in implementing efficient SPH simulations.

### A. Tree-based approach

In its simplest formulation, all particles in an SPH simulation have a constant smoothing length  $h$ . In such a setup, finding the particles in range of any other particle is similar to Molecular Dynamics simulations, in which all particles interact within a constant cutoff radius, and approaches which

are used in the latter, e.g. cell-linked lists [2] or Verlet lists [3] can be used [4], [5].

The neighbour-finding problem becomes more interesting, or difficult, in SPH simulations with variable smoothing lengths, i.e. in which each particle has its own smoothing length  $h_i$ , with ranges spanning up to several orders of magnitude. In such cases, e.g. in Astrophysics simulations [6], the above-mentioned approaches cease to work efficiently. Such codes therefore usually rely on *trees* for neighbour finding [7]–[9], i.e.  $k$ -d trees [10] or octrees [11] are used to decompose the simulation space. The particle interactions are then computed by traversing the list of particles and searching for their neighbours in the tree.

Using such trees, it is in principle trivial to parallelize the neighbour finding and the actual computation on shared-memory computers, e.g. each thread walks the tree for a different particle, identifies its neighbours and computes the densities and/or the second derivatives of the physical quantities for that particle.

Despite their simple and elegant formulation, the tree-based approach to neighbour-finding has three main problems:

- Computational efficiency: Finding all neighbours of a particle in the tree is, on average, in  $\mathcal{O}(\log N)$ , and worst-case behavior in  $\mathcal{O}(N^{2/3})$  [12], i.e. the cost per particle grows with the total number of particles  $N$ .
- Cache efficiency: When searching for the neighbours of a given particle, the data of all potential neighbours, which may not be contiguous in memory, is traversed separately.
- Symmetry: The parallel tree search can not exploit symmetry, i.e. a pair  $p_i$  and  $p_j$  will always be found twice, once when walking the tree for each particle.

These problems are all inherently linked to the use of spatial trees, i.e. more specifically their traversal, for neighbour-finding. As of here we will proceed differently, using a hierarchical cell decomposition, and computing the interactions by cell pairs, avoiding the above-mentioned problems.

### B. Spatial decomposition

If  $h_{\max} := \max_i h_i$  is the maximum smoothing length of any particle in the simulation, we start by splitting the simulation domain into rectangular cells of edge length larger or equal to  $h_{\max}$ .

Given such an initial decomposition, we then generate a list of cell *self-interactions*, which contains all non-empty cells in the grid. This list of interactions is then extended by the cell *pair-interactions*, i.e. a list of all non-empty cell pairs sharing either a face, edge, or corner. For periodic domains, cell pair-interactions need also be specified for cell neighbouring each other across periodic boundaries. These self- and pair-interactions encode, conceptually at least, the evaluation of the interactions between all particles in the same cell, or all interactions between particle pairs spanning a pair of cells, respectively.

In this first coarse decomposition, if a particle  $p_j$  is within range of a particle  $p_i$ , both will be either in the same cell, or

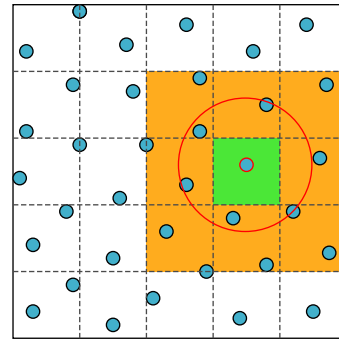


Fig. 1. Initial spatial decomposition: The simulation volume is divided into cells of edge length greater or equal to the largest smoothing length in the system. All neighbours of any given particle (small red circle) within that particle's smoothing length (large red circle) are guaranteed to lie either within that particle's own cell (green) or the directly adjacent cells (orange).

in neighbouring cells for which a cell self-interaction or cell pair-interaction has been specified respectively (see Figure 1).

In the best of cases, i.e. if each cell contains only particles with smoothing length equal to the cell edge length, if for any particle  $p_i$  we inspect each particle  $p_j$  in the same and neighbouring cells, only roughly 16% of the  $p_j$  will actually be within range of  $p_i$  [13], and is even worse if the cells contain particles whose smoothing length is less than the cell edge length. We therefore recursively refine the cell decomposition, bisecting each cell along all spatial dimension if: (a) The cell contains more than some minimal number of particles, and (b) the smoothing length of a reasonable fraction of the particles within the cell is less than half the cell edge length.

After the cells have been split, the cell self-interactions of each cell can be split up into the self-interaction of its sub-cells and the pair-interactions between them. Likewise, the cell pair-interactions between two cells that have been split can themselves be split up into the pair-interactions of the sub-cells spanning the original pair boundary if, and only if, all particles in both cells have a smoothing length of less than half the cell edge length (see Figure 2).

If the cells, self-interactions, and pair-interactions are split in such a way, if two particles are within range of each other, they will (a) either share a cell for which a cell self-interaction is defined, or (b) they will be located in two cells which share a cell pair-interaction. In order to identify all the particles within range of each other, it is therefore sufficient to traverse the list of self-interactions and pair-interactions and inspect the particle pairs therein.

### C. Particle interactions

The interactions between all particle pairs within a given cell, i.e. the cell's self-interaction, can be computed by means of a double `for`-loop over the cell's particle array. The algorithm, in C-like pseudo code, can be written as follows:

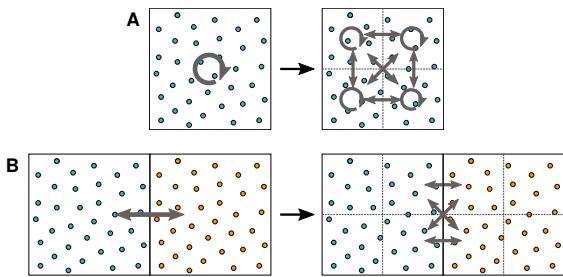


Fig. 2. **(A)** Large cells can be split, and their self-interaction replaced by the self- and pair-interactions of their sub-cells. **(B)** If all particles in a pair of interacting cells have a smoothing length less or equal to half of the cell edge length, both cells can be split, and their pair-interaction replaced by the pair-interactions of the neighbouring sub-cells across the interface.

```

1 for ( i = 0 ; i < count_i ; i++ ) {
2   for ( j = i+1 ; j < count ; j++ ) {
3     rij = ||parts[i] - parts[j]||.
4     if ( rij < h[i] || rij < h[j] ) {
5       compute interaction.
6     }
7   }
8 }

```

where `count` is the number of particles in the cell and `parts` and `h` refers to an array of those particles and their smoothing lengths respectively.

The interactions between all particles in a pair of cells can be computed similarly, e.g.:

```

1 for ( i = 0 ; i < count_i ; i++ ) {
2   for ( j = 0 ; j < count_j ; j++ ) {
3     rij = ||parts_i[i] - parts_j[j]||.
4     if ( rij < h_i[i] || rij < h_j[j] ) {
5       compute interaction.
6     }
7   }
8 }

```

where `count_i` and `count_j` refer to the number of particles in each cell and `parts_i` and `parts_j`, and `h_i` and `h_j`, refer to the particles of each cell and their smoothing lengths respectively.

As described in [13], using this naive double `for`-loop, for uniform particle distributions only 33.5%, 16.2%, and 3.6% of all particle pairs between cells sharing a common face, edge, or corner, respectively, will be within range of each other, leading to an excessive number of spurious pairwise distance evaluations (line 3). We will therefore use the sorted cell interactions described in [13] and [14], yet with some minor modifications, as the original algorithm is designed for systems in which the smoothing lengths of all particles are equal: We first sort the particles in both cells along the vector joining the centers of the two cells and then loop over the parts  $p_i$  on the left and interact them with the sorted parts  $p_j$  on the right which are within  $h_i$  along the cell pair axis. The same procedure is repeated for each particle  $p_j$  on the right, interacting with each other particle  $p_i$  on the left, which is within  $h_j$ , but not within  $h_i$ , along the cell pair axis (see Figure 3). The resulting algorithm, in C-like pseudo-code, can be written as follows:

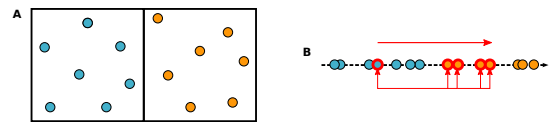


Fig. 3. Sorted cell pair-interactions. **(A)** Starting from a pair of neighbouring cells, **(B)** the particles from both cells are projected onto the axis joining the centers of the two cells. The particles on the left (blue) and right (orange) are then sorted in descending and ascending order respectively. Each particle on the left is then only interacted with the particles on the right within the cutoff radius along the cell axis.

```

1 for ( i = 0 ; i < count_i ; i++ ) {
2   for ( jj = 0 ; jj < count_j ; jj++ ) {
3     j = ind_j[jj];
4     if ( r_i[i] + h_i[i] < r_j[j] )
5       break;
6     rij = ||parts_i[i] - parts_j[j]||.
7     if ( rij < h_i[i] ) {
8       compute interaction.
9     }
10  }
11 }
12 for ( j = 0 ; j < count_j ; j++ ) {
13   for ( ii = count_i-1 ; ii >= 0 ; ii-- ) {
14     i = ind_i[ii];
15     if ( r_i[i] < r_j[j] - h_j[j] )
16       break;
17     rij = ||parts_i[i] - parts_j[j]||.
18     if ( rij < h_j[j] && rij > h_i[i] ) {
19       compute interaction.
20     }
21   }
22 }

```

where `r_i` and `r_j` contains the position the particles of both cells along the cell axis, and `ind_i` and `ind_j` contain the particle indices sorted with respect to these positions respectively.

This may seem like quite a bit of sorting, but if a cell has been split and its sub-cells have been sorted, the sorted indices of the higher-level cell can be constructed by shifting and merging the indices of its eight sub-cells. This reduces the  $\mathcal{O}(n \log n)$  sorting to  $\mathcal{O}(n)$  for merging. Furthermore, instead of sorting the particles every time we compute the pairwise interactions between two cells, we can pre-compute the sorted indices along the 13 possible cell-pair axes and store them for each cell, i.e. as is done in [14]. The sorted indices can also be re-used over several time steps until the hierarchical cell decomposition needs to be re-computed.

#### D. Parallel implementation

OpenMP [15] is arguably the most well-known paradigm for shared-memory, or multi-threaded parallelism. In OpenMP, compiler annotations are used to describe if and when specific loops or portions of the code can be executed in parallel. When such a parallel section, e.g. a parallel loop, is encountered, the sections of the loop are split statically or dynamically over the available threads, each executing on a single core, and merge at the end of the parallel section. Unfortunately, this can lead to a lot of inefficient branch-and-bound type operations, which generally lead to low performance and bad scaling on even moderate numbers of cores (see Figure 4).

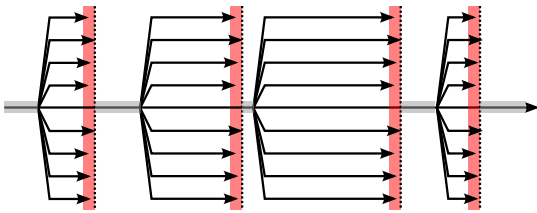


Fig. 4. Branch-and-bound parallelism as is commonly used in OpenMP. The horizontal arrows indicate the program flow over time, and branching arrows indicate a parallel section. The dotted vertical bars are the synchronization points at the end of each such section. Parallel efficiency is lost due to two factors: The grey shaded areas along the main horizontal area indicate parts of the program that do not execute in parallel and restrict the maximum parallel efficiency, e.g. as described by Amdahl's law, and the red areas indicate the difference between the fastest and slowest threads in each parallel block, i.e. the time lost to thread synchronization.

Furthermore, this form of shared-memory parallelism provides no implicit mechanism to avoid or handle concurrency problems, e.g. two threads attempting to modify the same data at the same time, or data dependencies between them. These must be implemented explicitly using either redundancy, barriers, critical sections, or atomic memory operations, which can further degrade parallel performance.

In order to better exploit shared-memory parallelism, we have to change the underlying paradigm, i.e. instead of annotating an essentially serial computation with parallel bits, it is preferable to describe the whole computation in a way that is inherently parallelizable. One such approach is *task-based parallelism*, in which the computation is divided into a number of inter-dependent computational tasks, which are then dynamically allocated to a number of processors. In order to ensure that the tasks are executed in the right order, e.g. that data needed by one task is only used once it has been produced by another task, and that no two tasks update the same data at the same time, constraints are specified and enforced by the task scheduler.

Several middle-wares providing such task-based parallelism exist, e.g. Cilk [16], QUARK [17], StarPU [18], SMP Super-scalar [19], OpenMP 3.0 [20], and Intel's TBB [21]. These implementations allow for the specification of individual tasks along with their *dependencies*, i.e. hierarchical relationships specifying which tasks must have completed before another task can be executed.

We will, however, differ from these approaches in that we introduce the concept of *conflicts* between tasks. Conflicts occur when two tasks operate on the same data, but the order in which these operations must occur is not defined. In previous task-based models, conflicts can be modeled as dependencies, yet this introduces an artificial ordering between the tasks and imposes unnecessary constraints on the task scheduler (e.g. mutual and non-mutual interactions in [22]). These conflicts can be modelled using exclusive *locks* on shared resources, i.e. a task will only be scheduled if it can obtain an exclusive lock on, and thus exclusive access to, potentially shared data.

The particle interactions described in the previous subsection lead to three basic task types:

- Cell *sorting*, in which the particles in a given cell are sorted with respect to their position along a one-dimensional axis,
- Cell *self-interaction*, in which all the particles of a given cell are interacted with all the other particles within the same cell,
- Cell *pair-interaction*, in which the interactions for all particle pairs spanning a pair of cells are computed.

The self-interaction and pair-interaction tasks exist in two flavors, one for the density computation and one for the force computation. Each pair-interaction task requires the sorted indices of the particles in each cell provided by the sorting tasks. Since the tasks are restricted to operating on the data of a single cell, or pair of cells, two tasks conflict if they operate on overlapping sets of cells. Due to the hierarchical nature of the spatial decomposition, two tasks also conflict if the cells of one task are sub-cells of the other.

Since the SPH computations have two phases, i.e. density and force computation, we introduce a *ghost* task in between for each cell. This ghost task depends on all the density computations for a given cell, and, in turn, all force computations involving that cell depend on its ghost task. Using this mechanism, we can enforce that all density computations for a set of particles have completed before we use this density in the force computations.

The dependencies and conflicts between tasks can thus be formulated as follows:

- A cell sorting task on a cell with sub-cells depends on the sorting tasks of all its sub-cells.
- A cell pair-interaction depends on the cell sorting tasks of both its cells.
- Cell pair-interaction and cell self-interaction tasks operating on overlapping sets of cells or sub-cells conflict with each other.
- The ghost task of each cell depends on all the density cell pair interactions and self-interactions which involve the particles in that cell.
- The ghost task of each cell depends on the ghost tasks of its sub-cells.
- The force cell pair-interaction and self-interaction tasks depend on the ghost tasks of the cells on which they operate.

These task dependencies are illustrated in Figure 5.

This task decomposition has significant advantages over the use of spatial trees: First of all, the cost of identifying all particles in range of a given particle does not depend on the total number of particles. Furthermore, the particle interactions in each task are computed symmetrically, i.e. each particle pair is identified only once for each interaction type. The sorted particle indices can be re-used for both the density and force computation, and over several time-steps, thus reducing the computational cost even further. Finally, if the particles are stored grouped by cell, each task then only involves accessing

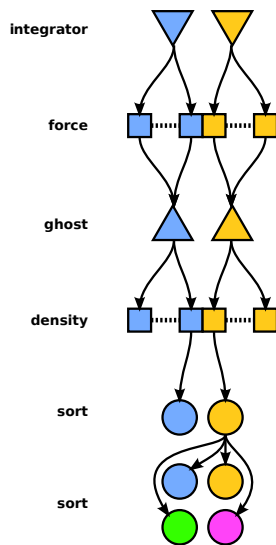


Fig. 5. Task dependencies and conflicts: Arrows indicate the dependencies between different task types, i.e. an arrow from task A to task B indicates that A depends on B. Horizontal dashed lines between tasks indicate conflicts, i.e. the two tasks can not be executed concurrently. Each sort task (circles) depends only on the sort tasks of its sub-cells. The pair-interactions (rectangles) for the particle density computation depend on the sort tasks of the respective cells, whereas self-interaction tasks (squares) for the density computation do not, as they do not require sorting. Self- and pair-Interactions on overlapping cells (same colour) conflict with each other. The ghost task of each cell (triangles) depends on the self- and pair-interaction density tasks. The self- and pair-interaction tasks for the force computation, finally, depend on the ghost tasks of the respective cells.

and modifying a contained and contiguous regions of memory, thus potentially improving cache re-use [23].

### III. VALIDATION

In the following, we describe how the algorithms shown in the previous section are implemented and tested against existing codes on specific test problems.

#### A. Implementation details

The algorithms described above are all implemented as part of SWIFT (SPH With Inter-dependent Fine-grained Tasking), an Open-Source platform for hybrid shared/distributed-memory SPH simulations<sup>1</sup>.

SWIFT is implemented in C, and can be compiled with the gcc compiler. Although SIMD-vectorized code, using the gcc vector types and SSE/AVX intrinsics, has been implemented, it was switched off in the following to allow for a fair comparison against unvectorized codes.

The code for the task-based parallelism is implemented using standard pthreads [24], and in some places, e.g. in the time-stepper or task list creation, OpenMP is used. Each thread is assigned its own task queue, over which the tasks are distributed evenly in topological order of the dependencies. If a thread runs out of tasks, it can steal from another task's queue [25]. The threads are initialized once at the start of the simulation and synchronize via a barrier between time steps.

<sup>1</sup>See <http://swiftsim.sourceforge.net/>

#### B. Simulation setup

In order to test their accuracy, efficiency, and scaling, the algorithms described in the previous section were tested in SWIFT using the following three simulation setups:

- *Sod-shock* [26]: A cubic periodic domain containing a high-density region of 800 000 particles with  $P_i = 1$  and  $\rho_i = 1$  on one half, and a low-density region of 200 000 particles with  $P_i = 0.1795$  and  $\rho_i = 1/4$  on the other.
- *Sedov blast*: A cubic grid of  $101 \times 101 \times 101$  particles at rest with  $P_i = 10^{-5}$  and  $\rho_i = 1$ , yet with the energy of the central 33 particles set to  $u_i = 100/33/m_i$ .
- *Cosmological volume*: Realistic distribution of matter in a periodic volume of universe. The simulation consists of 1 841 127 particles with a mix of smoothing lengths spanning three orders of magnitude, providing a test-case for neighbour finding and parallel scaling in a real-world scenario.

The first two cases are used both for benchmarking and for validating the correctness of the code. In all simulations, the constants  $N_{ngb} = 48$ ,  $\gamma = 5/3$ ,  $C_{CFL} = 0.3$ , and  $\alpha = 2.0$  (viscosity) were used. In SWIFT, cells were split if they contained more than 400 particles and more than 87.5% of the particles had a smoothing length less than half the cell edge length.

In all three test cases, results were computed using a fixed time step and updating the forces on all particles in each time-step.

The simulation results were compared with Gadget-2 [8] in terms of speed and parallel scaling. Gadget-2 was compiled with the Intel C Compiler version 2013.0.028 using the options `-DUSE_IRECV -O3 -ip -fp-model fast -ftz -no-prec-div -mcmmodel=medium`. For the parallel runs, OpenMPI version 1.6.3 was used [27].

SWIFT v. 0.1.0 was compiled with the GNU C Compiler version 4.7.2 using the options `-O3 -ffast-math -fstrict-aliasing -ftree-vectorize -funroll-loops -m32 -msse -msse2 -msse3 -mssse3 -msse4.1 -msse4.2 -mavx -fopenmp -march=native -pthread`. Note that although the compiler switches for the SSE and AVX vector instruction sets were activated, explicit SIMD-vectorization was not used.

All simulations were run on a 4×Intel Xeon E5-4640 32-core machine running at 2.4GHz with CentOS release 6.2 Linux for x86\_64.

#### C. Results

The scaling and efficiency of SWIFT for the simulations described in the previous subsection are shown in Figure 6. In all three cases, SWIFT obtains a parallel efficiency of over 75% on 32 cores. For the Cosmological volume, it is also more than eight times faster than Gadget-2.

Figure 7 shows the total contribution of each task type, as well as the overheads for task acquisition and time integration for the Cosmological volume simulation. Note that efficiency is lost principally in the self and pair interactions, which is

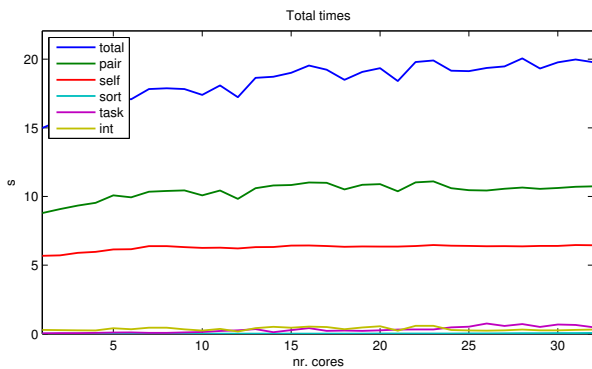


Fig. 7. Total time for each task type, plus overheads for task management and time integration. The values, in seconds, are summed over all processors.

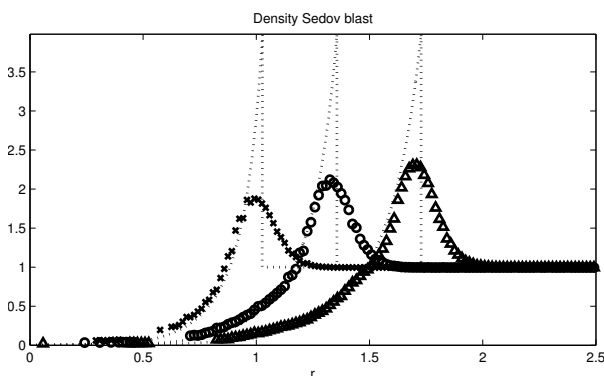


Fig. 8. Average radial density profiles and analytical solutions (dotted lines) for the Sedov blast simulation at times  $t = \{0.075, 0.15, 0.275\}$ .

most probably due to the reduction of the effective memory bandwidth with the increasing number of cores used. The overheads for task acquisition contribute less than 3.5% to the total costs.

In order to assess the correctness of the simulation, average radial density, pressure, and velocity profiles were computed for the Sedov blast (see Figure 8) and Sod-shock (see Figure 9) simulations and compared with the analytical results given in [28] and [26] respectively. These results are comparable to the output produced by Gadget-2 for the same initial conditions, and sharper results could be achieved at higher resolutions and/or different parameterizations.

#### IV. CONCLUSIONS

The results show that SWIFT is significantly more efficient than current state-of-the-art tree-based methods. The improved performance is the result of several features:

- Cell-based neighbour searching which requires only constant time per particle,
- Sorted particle interactions which significantly reduce the number of spurious pairwise distance computations in the neighbour search,
- Use of symmetry in computing the particle densities and forces, thus requiring each particle pair to be found only

once,

- Better cache efficiency of the cell-based interactions.

Since no hardware-specific tricks or explicit SIMD-vectorization were used, although the latter is available in the code, they can not be made responsible for the improved efficiency.

In addition to the increased speed, SWIFT also shows good scaling, in excess of 75% parallel efficiency on 32 cores, for all three simulations. This is due to the fine-grained load balancing and low number of synchronization points as a result of the task-based parallelism scheme.

We are currently working to extend SWIFT for hybrid shared/distributed-memory parallelism, and to GPUs [29]. Task-based parallelism will play an important role for both these developments: In hybrid schemes, asynchronous communication between distributed-memory nodes can be modelled as simply another set of tasks with their corresponding dependencies, thus avoiding excessive synchronization points or latencies. As has already been shown for molecular dynamics simulations, the task-based parallel scheme can also easily be extended for computations on GPUs, using the same set of tasks and dependencies. Work is also ongoing in adding different and better implementations of particle-based hydrodynamics, i.e. for cosmological simulations [30].

#### ACKNOWLEDGMENTS

The authors would like to thank Lydia Heck of the Institute for Computational Cosmology, Durham University, for having initiated this interdisciplinary collaboration, and for providing exclusive access to the hardware on which all benchmarks were run.

#### REFERENCES

- [1] M. Snir, S. Otto, S. Huss-Lederman, D. Walker, and J. Dongarra, *MPI: The Complete Reference (Vol. 1): Volume 1-The MPI Core*. MIT press, 1998, vol. 1.
- [2] M. Allen and D. Tildesley, *Computer simulation of liquids*. Oxford university press, 1989, vol. 18, no. 195.
- [3] L. Verlet, "Computer "experiments" on classical fluids. I. Thermodynamical properties of Lennard-Jones molecules," *Physical Review*, vol. 159, no. 1, p. 98, 1967.
- [4] J. Domínguez, A. Crespo, M. Gómez-Gesteira, and J. Marongiu, "Neighbour lists in smoothed particle hydrodynamics," *International Journal for Numerical Methods in Fluids*, vol. 67, no. 12, pp. 2026–2042, 2011.
- [5] G. Viccione, V. Bovolín, and E. P. Carratelli, "Defining and optimizing algorithms for neighbouring particle identification in sph fluid simulations," *International Journal for Numerical Methods in Fluids*, vol. 58, no. 6, pp. 625–638, 2008.
- [6] R. A. Gingold and J. J. Monaghan, "Smoothed particle hydrodynamics-theory and application to non-spherical stars," *Monthly notices of the royal astronomical society*, vol. 181, pp. 375–389, 1977.
- [7] L. Hernquist and N. Katz, "TREESPH-A unification of SPH with the hierarchical tree method," *The Astrophysical Journal Supplement Series*, vol. 70, pp. 419–446, 1989.
- [8] V. Springel, "The cosmological simulation code Gadget-2," *Monthly Notices of the Royal Astronomical Society*, vol. 364, no. 4, pp. 1105–1134, 2005.
- [9] J. Wadsley, J. Stadel, and T. Quinn, "Gasoline: a flexible, parallel implementation of TreeSPH," *New Astronomy*, vol. 9, no. 2, pp. 137–158, 2004.
- [10] J. L. Bentley, "Multidimensional binary search trees used for associative searching," *Communications of the ACM*, vol. 18, no. 9, pp. 509–517, 1975.

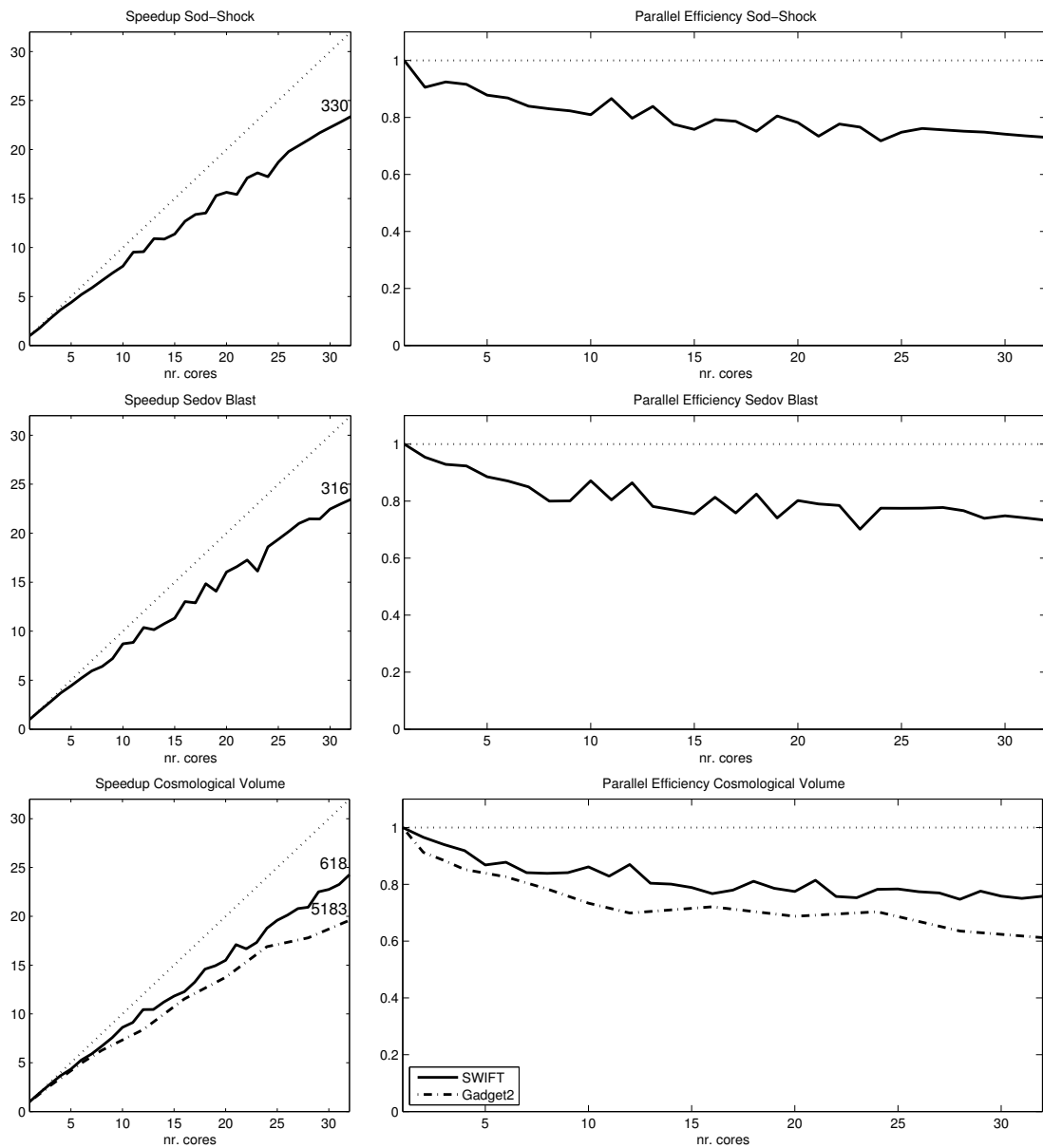


Fig. 6. Parallel scaling and efficiency for the Sod-shock, Sedov blast Cosmological volume simulations. The numbers in the scaling plots indicate the average milliseconds per time step when running on all 32 cores.

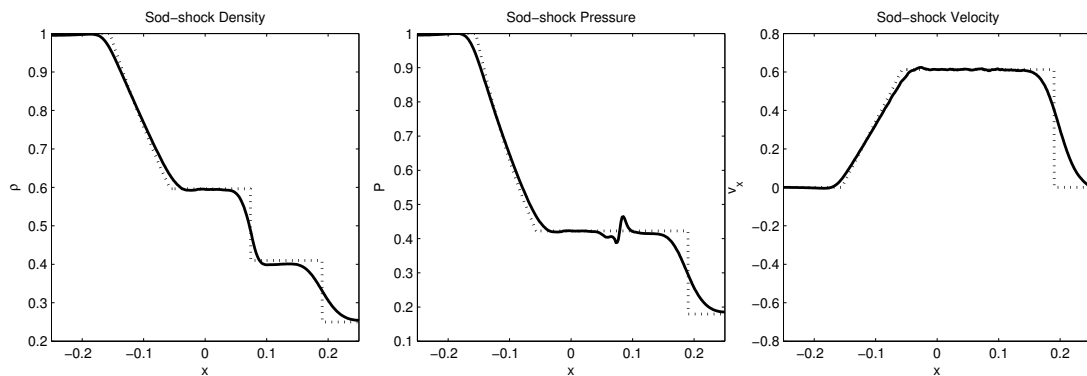


Fig. 9. Average density, pressure, and velocity in  $x$ -direction, along with the corresponding analytical solutions (dotted lines) for the Sod-shock simulations at  $t = 0.12$ .

- [11] D. Meagher, "Geometric modeling using octree encoding," *Computer Graphics and Image Processing*, vol. 19, no. 2, pp. 129–147, 1982.
- [12] D.-T. Lee and C. Wong, "Worst-case analysis for region and partial region searches in multidimensional binary search trees and balanced quad trees," *Acta Informatica*, vol. 9, no. 1, pp. 23–29, 1977.
- [13] P. Gonnet, "A simple algorithm to accelerate the computation of non-bonded interactions in cell-based molecular dynamics simulations," *Journal of Computational Chemistry*, vol. 28, no. 2, pp. 570–573, 2007.
- [14] —, "Pseudo-Verlet lists: A new, compact neighbor list representation," *Molecular Simulation*, vol. in press, 2013.
- [15] L. Dagum and R. Menon, "OpenMP: an industry standard API for shared-memory programming," *Computational Science & Engineering, IEEE*, vol. 5, no. 1, pp. 46–55, 1998.
- [16] R. Blumofe, C. Joerg, B. Kuszmaul, C. Leiserson, K. Randall, and Y. Zhou, *Cilk: An efficient multithreaded runtime system*. ACM, 1995, vol. 30, no. 8.
- [17] A. YarKhan, J. Kurzak, and J. Dongarra, *QUARK Users' Guide*, Electrical Engineering and Computer Science, Innovative Computing Laboratory, University of Tennessee, April 2011.
- [18] C. Augonnet, S. Thibault, R. Namyst, and P.-A. Wacrenier, "StarPU: A unified platform for task scheduling on heterogeneous multicore architectures," *Concurrency and Computation: Practice and Experience, Special Issue: Euro-Par 2009*, vol. 23, pp. 187–198, 2011. [Online]. Available: <http://hal.inria.fr/inria-00550877>
- [19] *SMP Superscalar (SMPSS) User's Manual, Barcelona Supercomputing Center*, 2008.
- [20] A. Duran, R. Ferrer, E. Ayguadé, R. M. Badia, and J. Labarta, "A proposal to extend the OpenMP tasking model with dependent tasks," *International Journal of Parallel Programming*, vol. 37, no. 3, pp. 292–305, 2009.
- [21] J. Reinders, *Intel threading building blocks: outfitting C++ for multi-core processor parallelism*. O'Reilly Media, Incorporated, 2007.
- [22] H. Ltaief and R. Yokota, "Data-driven execution of fast multipole methods," *arXiv preprint arXiv:1203.0889*, 2012.
- [23] E. S. Fomin, "Consideration of data load time on modern processors for the Verlet table and linked-cell algorithms," *Journal of Computational Chemistry*, vol. 32, no. 7, pp. 1386–1399, 2011.
- [24] I. P. A. S. Committee *et al.*, "IEEE Std 1003.1 c-1995, threads extensions," 1995.
- [25] R. D. Blumofe and C. E. Leiserson, "Scheduling multithreaded computations by work stealing," *Journal of the ACM (JACM)*, vol. 46, no. 5, pp. 720–748, 1999.
- [26] G. A. Sod, "A survey of several finite difference methods for systems of nonlinear hyperbolic conservation laws," *Journal of Computational Physics*, vol. 27, no. 1, pp. 1–31, 1978.
- [27] E. Gabriel, G. Fagg, G. Bosilca, T. Angskun, J. Dongarra, J. Squyres, V. Sahay, P. Kambadur, B. Barrett, A. Lumsdaine *et al.*, "Open MPI: Goals, concept, and design of a next generation MPI implementation," *Recent Advances in Parallel Virtual Machine and Message Passing Interface*, pp. 353–377, 2004.
- [28] L. Sedov, "Similarity and dimensional methods in mechanics (similarity and dimensional methods in mechanics, new york," 1959.
- [29] A. B. G. Chalk and P. Gonnet, "Using task-based parallelism directly on GPUs," Submitted to SC13 Supercomputing Conference, 2013.
- [30] M. Schaller, R. Bower, and T. Theuns, "On the use of particle based methods for cosmological hydrodynamical simulations," in *8th International SPHERIC Workshop*, 2013.